Available online at www.sciencedirect.com
SCIENCE DIRECT®
Chemical Physics 286 (2003) 205–217
Chemical Physics
www.elsevier.com/locate/chemphys

DFT study of hydrogen-bonded dimers and tetramer of glyoxilic acid oxime

Ivelina Georgieva[a], Daniel Binev[a], Natasha Trendafilova[a,*], Günther Bauer[b]

[a] *Institute of General and Inorganic Chemistry, Bulgarian Academy of Sciences, Sofia BG-1113, Bulgaria*
[b] *Institute of Chemical Technologies and Analytics, Technical University of Vienna, Vienna A-1060, Austria*

Received 3 July 2002

Abstract

DFT study of hydrogen-bonded dimers and tetramer of glyoxilic acid oxime (GAO) has been performed at B3LYP/6-31G* and B3LYP/6-31++G** levels of the theory. The N···H—O and O···H—O hydrogen bondings in the self-assembling structures studied have been estimated from intermolecular distances, enthalpy of stabilization, hydrogen-bonding energies and AIM electron density at the hydrogen bond critical points. The calculated hydrogen-bonding energies of various GAO dimers suggested a cooperative interaction in the cyclic dimers and tetramer. The comparative study of chain aggregate with both head-to-head and tail-to-tail bondings and chain aggregate only with head-to-tail bondings, showed that the latter is enthalpically preferred in agreement with the crystal structure of GAO. Harmonic frequencies for the monomer, five dimers and tetramer have been calculated and discussed as to the changes in the most sensitive to the complexation vibrations and as to the strengths of the O···H—O and N···H—O hydrogen bondings. Vibrational analysis at B3LYP/6-31G* level confirmed the suggestion for a cooperativity in the cyclic H-bonded complexes. Natural population analysis was performed to predict electrostatic interactions in the cyclic H-bonded complexes. The π-delocalization was estimated on the basis of the calculated AIM ellipticity.

Keywords: Glyoxilic acid oxime; Cyclic H-bonded complexes; Hydrogen-bonding energy; Cooperativity; DFT study

1. Introduction

The glyoxilic acid oxime (HOOC—CH—NOH) (GAO) has two donor atoms, the carboxyl oxygen and the oxime nitrogen and it can act as a mono- or bi-dentate ligand in a series of metal complexes [1]. The presence of electron-rich centers (=N, =O) and hydrogen atoms covalently bonded to electronegative atoms provides the possibility of forming different type intermolecular hydrogen bonds, O···H—O and N···H—O. Although the compound was synthesized in 1910 [2] structural data were not found in the literature. In our previous studies we performed detailed conformational study of the glyoxilic acid oxime and its anions at different levels of the theory, HF/6-311G**, MPn/6-311G** ($n = 2, 3, 4$) and B3LYP/

* Corresponding author. Tel.: +1-359-2-9792592; fax: +1-359-2-705024.
E-mail address: ntrend@svr.igic.bas.bg (N. Trendafilova).

0301-0104/03/$ - see front matter © 2002 Elsevier Science B.V. All rights reserved.
PII: S0301-0104(02)00938-2

6-311G** [3]. HF and MPn calculations predicted the ectt as the lowest energy conformer, followed by ecct, ettt and zccc (Fig. 1). Density functional theory, however, suggested strong intramolecular H-bond (O···H—O) in zccc conformer and energetic preference to this conformer. Since the solid state vibrational spectrum of GAO was in best agreement with ectt, but not with zccc spectral features [3], we suggested that ectt conformer is realized in the solid state and in the complexes we obtained [1]. Recently we succeeded in obtaining crystals of good quality and GAO crystal structure was determined by X-ray diffraction analysis [4]. The results showed that in crystal four molecules are held together by O···H—O and N···H—O interactions as shown in Fig. 2 [4]. All four molecules in the cyclic tetramer have the predicted ectt conformation [3] but they undergoes head-to-tail hydrogen bonding and form a four-membered hydrogen-bonded, almost planar ring. The study of the formation of self-assembling structures that lead to crystallization provides a useful and convenient means to evaluate the importance of the intermolecular interactions [5]. Understanding

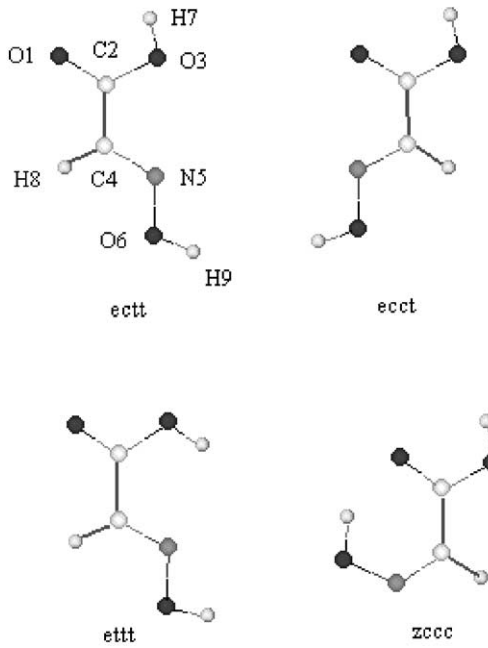

Fig. 1. Low energy conformers of the glyoxilic acid oxime.

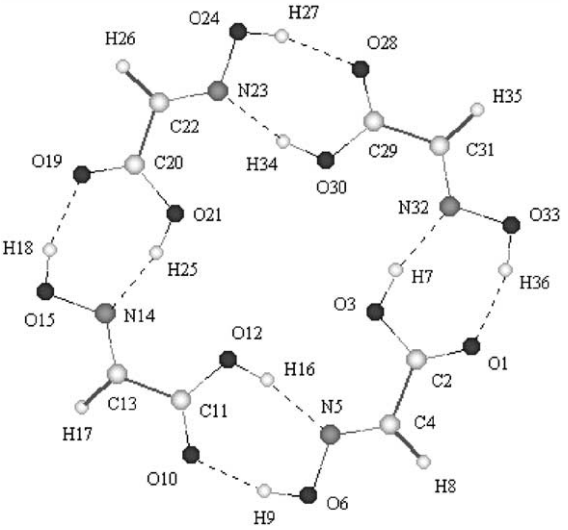

Fig. 2. Cyclic tetramer of the glyoxilic acid oxime.

these interactions and their cooperative effects can also have important consequences for studies of molecular recognition [6–9]. In this study we apply density functional theory method to gain a deeper insight into the nature of the intermolecular interactions that bind the ectt monomer units in the glyoxilic acid oxime tetramer. The analysis made allowed us to estimate the strengths of the O···H—O and N···H—O hydrogen bondings leading to tetramer formation of GAO, as well as to evaluate the cooperativity in the cyclic dimers and tetramer complexes.

2. Computational procedures

DFT calculations were performed using GAUSSIAN 98 package [10]. Density functional theory was used with Becke3-Lee-Yang-Parr (B3-LYP) exchange-correlation functional and 6-31G* and 6-31++G** basis sets [11,12]. According to recent reports only hybrid functionals can provide an accurate description for the systems with hydrogen bonds [13–16]. All geometries were completely optimized at the levels of calculations noted. Vibrational frequencies were calculated to verify the nature of the stationary points found on the potential energy surface. The hydrogen-bonding

energy of the studied dimers and tetramer was corrected both with basis set superposition error (BSSE) and zero-point vibrational energies (ZPVE). The BSSE was estimated using the counterpoise (CP) method as described previously [17–20]

$$\Delta(\mathrm{BSSE}) = \sum_{i}^{n} (Em_{\mathrm{f}}^{i} - Em_{\mathrm{f}}^{i*}), \tag{1}$$

where the Em_{f}'s represent the energies of the individual monomers frozen in their aggregate geometries; the asterisk (*) denote monomers calculated with 'ghost' orbitals. The hydrogen-bonding enthalpies ($\Delta H_{\mathrm{complex}}$) were obtained from the calculated hydrogen-bonding energies $\Delta E_{\mathrm{complex}}$ as described in the literature [21–23]

$$\Delta H_{\mathrm{complex}} = \Delta E_{\mathrm{complex}}^{\mathrm{cp}} + \Delta E_{\mathrm{vib}} - 4RT, \tag{2}$$

where R is the gas constant.

A topological analysis of the B3LYP/6-31G* electron density at bonds was performed with Bader's atoms in molecules (AIM) theory to describe the electronic structures of the dimers and tetramer of GAO [24–27]. The calculated electron density, ρ_{b}, and its second derivative, $\nabla^2\rho_{\mathrm{b}}$ (Laplacian), at hydrogen bond critical points can characterize the intermolecular homo- (O···H—O) and heteronuclear (N···H—O) bondings in the species studied. The Laplacian of the electron density was used to study the σ- and π-bond character in the GAO dimers and tetramer, which can be quantified by means of the bond ellipticity ε. The AIM calculations were performed using the critical point option for the AIM keyword as implemented in GAUSSIAN 98.

The harmonic frequency shift of the O—H stretching mode in dimer and tetramer, $\Delta\nu_{\mathrm{O-H}}$, was estimated using the equation

$$\Delta\nu_{\mathrm{O-H\ complex}} = \nu_{\mathrm{O-H\ complex}}((\mathrm{N})\mathrm{O}\cdots\mathrm{H}\text{—}\mathrm{O}) - \nu_{\mathrm{O-H(monomer)}} \tag{3}$$

The vibrational spectra were calculated at the optimized geometries of monomer, dimers and tetramer at DFT(B3LYP)/6-31G* level of the theory. In order to assign the calculated frequencies to approximate vibrational descriptor, the vibrational modes have been analyzed by means of the atom movements, calculated in Cartesian coordinates. To improve the frequency shift estimation, corresponding 'optimal' scale factors were used as it was proposed in the literature [28,29]. The 'optimal' scale factors were determined using the ratio $\nu^{\mathrm{exp}}/\nu^{\mathrm{calc}}$. The predicted frequency shift for each vibration was defined as follows:

$$\Delta\nu^{\mathrm{scal}} = k_i(\nu_i^{\mathrm{tetramer}} - \nu_i^{\mathrm{monomer}}), \tag{4}$$

where k_i is the corresponding 'optimal' scale factor.

3. Results and discussion

3.1. Geometry parameters of tetramer, dimer I and monomer

The calculated geometry parameters of GAO tetramer (Fig. 2) are compared with available experimental data in Table 1. Since the tetramer has two equivalent dimer pairs (dimer I, Fig. 3) structural parameters only for one of them are presented in Table 1. The average deviations of the calculated bond lengths and bond angles are 5.1% and 1.4% at B3LYP/6-31G*, respectively and 5.3% and 0.8% at B3LYP/6-31++G**, respectively. Both levels predicted shorter N···H and O···H distances as compared to experiment. However, taking into account the low accuracy of the X-ray analysis in determining the H positions, the values of the experimental O···H and N···H distances should also be considered with caution [30]. On the other side, since the O—H vibration is very anharmonic, the minimum on the potential energy surface does not define precisely the position of the H atoms. Therefore, the experimental O···O and O···N distances were used to obtain information about the hydrogen-bonding strength in the complexes studied. As described in the literature, the O···O and N···O distances correlate with the hydrogen-bonding strengths and can supply reliable information about the intermolecular interactions in hydrogen-bonded systems [20,31,32]. As seen from Table 1, B3LYP/6-31G* calculations gave better coincidence with the experimental N···O and O···O distances with comparatively small deviations, ~0.02 and ~0.05 Å, respectively. These deviations could be overcome when a CP-optimization is performed. As it was shown the

Table 1
Selected structural parameters[a] of GAO monomer, dimer I and tetramer at B3LYP level and experimental data of GAO tetramer; distances (R) in Å and angles (A-valence) in degrees

Name definition[b]	B3LYP/6-31++G**	B3LYP/6-31G*			Experiment [4]
	Tetramer	Monomer	Dimer I	Tetramer	Tetramer
$R(C_2{=}O_1)$	1.233	1.214	1.213	1.230	1.2065(13)
$R(C_{11}{=}O_{10})$	1.233		1.232	1.230	1.2123(13)
$R(C_2{-}O_3)$	1.322	1.350	1.353	1.324	1.3165(13)
$R(C_{11}{-}O_{12})$	1.322		1.321	1.323	1.3132(14)
$R(C_2{-}C_4)$	1.482	1.483	1.480	1.482	1.4762(18)
$R(C_{11}{-}C_{13})$	1.482		1.482	1.482	1.4722(16)
$R(O_3{-}H_7)$	1.002	0.976	0.975	1.003	0.89(2)
$R(O_{12}{-}H_{16})$	1.002		1.000	1.002	0.865(18)
$R(C_4{=}N_5)$	1.282	1.280	1.282	1.281	1.2638(16)
$R(C_{13}{=}N_{14})$	1.282		1.280	1.281	1.2647(14)
$R(C_4{-}H_8)$	1.088	1.089	1.088	1.088	0.94(2)
$R(C_{13}{-}H_{17})$	1.088		1.089	1.088	0.94(2)
$R(N_5{-}O_6)$	1.357	1.385	1.356	1.355	1.3727(14)
$R(N_{14}{-}O_{15})$	1.357		1.383	1.355	1.3750(12)
$R(O_6{-}H_9)$	0.994	0.972	0.997	0.995	0.91(2)
$R(O_{15}{-}H_{18})$	0.994		0.972	0.996	0.93(2)
$R(N_5 \cdots H_{16})$	1.788		1.839	1.812	1.96(2)
$R(N_{14} \cdots H_{25})$	1.788			1.803	1.93(2)
$R(O_{10} \cdots H_9)$	1.744		1.724	1.756	1.92(2)
$R(O_{19} \cdots H_{18})$	1.745			1.755	1.90(2)
$R(N_5 \cdots O_{12})$	2.768		2.817	2.786	2.8025(16)
$R(N_{14} \cdots O_{21})$	2.768			2.781	2.7946(17)
$R(O_6 \cdots O_{10})$	2.708		2.696	2.718	2.7809(15)
$R(O_{15} \cdots O_{19})$	2.709			2.720	2.7736(17)
$A(O_{10}{=}C_{11}{-}O_{12})$	124.9	123.6[c]	125.2	125.4	124.64(10)
$A(C_{11}{-}O_{12}{-}H16)$	110.3	105.5[c]	109.2	109.5	108.5(10)
$A(C_4{=}N_5{-}O_6)$	115.1	111.2	114.6	115.4	113.2(10)
$A(C_2{-}C_4{-}H_8)$	118.3	116.4	117.5	118.7	117.0(12)
$A(O_{10}{=}C_{11}{-}C_{13})$	120.4	122.2[c]	119.3	120.2	120.56(10)
$A(C_2{-}C_4{=}N_5)$	118.7	120.6	120.0	118.1	118.77(11)
$A(O_{12}{-}C_{11}{-}C_{13})$	114.7	114.2[c]	115.5	114.3	114.8(9)

[a] The full set of the calculated (at B3LYP/6-31G*) valence and dihedral angles of GAO monomer, dimer I and tetramer can be obtained from the authors on request.
[b] See Figs. 1–3 for numbering of atoms.
[c] The values refer to corresponding angles in monomer in Fig. 1.

CP-optimized structures showed about 0.03 Å longer $O \cdots O$ distances in comparison with the 'normal' optimized ones [20]. Since the B3LYP/6-31G* calculations gave better coincidence of the $O \cdots O$ and $N \cdots O$ distances with the experimental ones, further the results obtained at this level of the theory will be commented.

The comparison between the geometrical parameters of monomer (ectt, Fig. 1) and dimer I (Fig. 3) showed that the hydrogen bonding of two monomers in a cyclic dimer I provoked substantially changes of the monomer bond lengths and angles, included in the seven-membered H-bonded ring. The $C_{11}{=}O_{10}$, $O_{12}{-}H_{16}$, $O_6{-}H_9$ bond lengths in dimer I are with 0.018–0.025 Å longer, while the $C_{11}{-}O_{12}$ and $N_5{-}O_6$ bond lengths are with 0.029 Å shorter. The longer C=O and the shorter C—O bonds in dimer indicated higher delocalization in the hydrogen-bonded carboxylic group, which contributes to the stability of the cyclic dimer structure. Due to the formation of seven-membered hydrogen-bonded ring, the O=C—O, C—O—H,

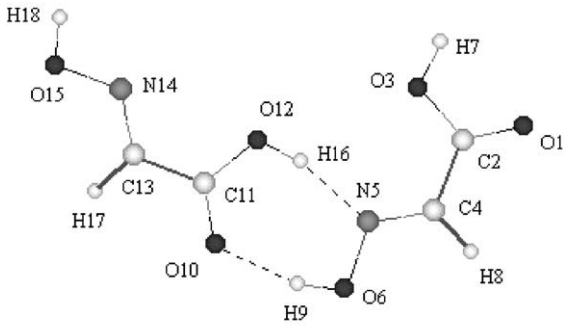

I

Fig. 3. Dimer I of the glyoxilic acid oxime.

C=N—O and C—C—H bond angles increased and the O=C—C bond angle decreased (with ~2–4°) as compared to the monomer (Table 1). The structural changes obtained in the seven-membered ring of dimer I were observed in the cyclic tetramer as well. Some additional changes, however, should be mentioned. The O···O distances in tetramer become longer and the N···O-shorter (Table 1). Obviously, the formation of cyclic tetramer complex decreased the difference between the N···O and O···O distances, as it was found from the experiment (Table 1). Thus, it is expected that in tetramer the N···H—O bonding become stronger and approaches the O···H—O one. More precise estimation of the N···H—O and O···H—O bonding strengths in tetramer will be done below on the basis of the calculated hydrogen-bonding energy and AIM electron density at the hydrogen bond critical points. As a result of the geometric constraints in the hydrogen-bonded seven-membered rings both dimer I and tetramer optimized geometries showed marked deviations from the idealized 180° (N)O···H—O angles (in dimer: $\angle$O···H—O = 163.8°, $\angle$N···H—O = 165.0°; tetramer: $\angle$O···H—O = 161.5°, $\angle$N···H—O = 163.0°). In addition, due to the tetramer cyclic formation, the O=C—C and C=N—O bond angles increased with ~1° and the O—C—C and C—C=N bond angles decreased with 1° and 2°, respectively (Table 1). The comparative study of the structural parameters of monomer, dimer I and tetramer showed that all the geometry changes observed are in the direction necessary to convert the geometry calculated for the isolated molecule to that experimentally observed for the crystal. Thus, it was found that the calculated structural parameters for tetramer are in best agreement with the experimental values of GAO.

3.2. Thermodynamic parameters

The total energies and thermodynamic parameters for hydrogen-bond formation of dimer I and tetramer, calculated at B3LYP/6-31++G** and B3LYP/6-31G* levels, are presented in Table 2. Both methods showed that the enthalpy and the free energy decreased going from dimer I to tetramer and thus pointed out stronger hydrogen-bonding interaction in self-assembling structures greater than dimer. The lower ΔG^0 values for tetramer indicated that the aggregation occurred although it is enthropically unfavored. In order to trace the GAO aggregation, we included the trimer unit in the consideration. As seen from Table 2, the calculated incremental hydrogen-bonding enthalpy of the second hydrogen bonding in trimer (−56.63 kJ/mol) is lower than the hydrogen-bonding enthalpy of the first one (that of dimer I, −55.63 kJ/mol). The results thus obtained showed that the formation of larger than dimer aggregate for GAO is enthalpically favored. This finding is in agreement with the suggestion given previously in the literature [6] that the interaction energy between two individual molecules is less enthalpically stabilizing than that between an aggregate and an individual molecule. As it was supposed, the crystal formation must start as a dimer, become a trimer and continue to add individual units or small aggregates until it has acquired enough three-dimensional supermolecular structure to be considered a crystal. It seems, that in such an aggregation process the cooperativity play an important role in the interaction energies of adding individual units to the growing aggregate [6].

3.3. Hydrogen-bonding energies and cooperativity in the cyclic complexes

In GAO tetramer one can trace four identical hydrogen-bonded rings (Fig. 2). In each ring par-

Table 2
Total energies and thermodynamic parameters for hydrogen-bond formation of GAO dimer I and tetramer

Method	System	Total energies (hartrees)	ΔS^0 (J mol^{-1} K^{-1})	ΔH^0 at 298.15 K (kJ mol^{-1})	ΔG^0 (kJ mol^{-1})
B3LYP/6-31++G**	Dimer I	−716.8465419	−155.90	−53.19	−6.71
	Tetramer	−1433.7414668	−549.21	−197.22	−33.47
B3LYP/6-31G*	Dimer I	−716.7817870	−155.96	−55.63	−9.13
	Trimer[a]	–	−155.62	−56.63	−10.23
	Tetramer	−1433.6185656	−545.97	−198.74	−35.96

[a] Incremental values for the second hydrogen bonding.

ticipate two molecules: each one acts both as a hydrogen-bonding donor and acceptor. To estimate the individual N···H—O and O···H—O bonding energies in tetramer, different dimer models were studied (Figs. 3–7). The uncorrected and corrected (with BSSE and ZPVE corrections) hydrogen-bonding energies of dimers I–V and tetramer at B3LYP/6-31G* and B3LYP/6-31++G** levels of theory, are collected in Table 3. After correction for ZPVE and basis set superposition errors, both methods predicted similar H-bonding energies for the studied dimers and tetramer. As described in the literature, the comparison of the BSSE corrections for the methods used showed that the enlargement of the basis set (with diffuse functions) leads to decrease of the BSSE values [9,33]. The BSSE's correction for the self-assembling structures studied is in the range 5–12% of the H-bonding energy at B3LYP/

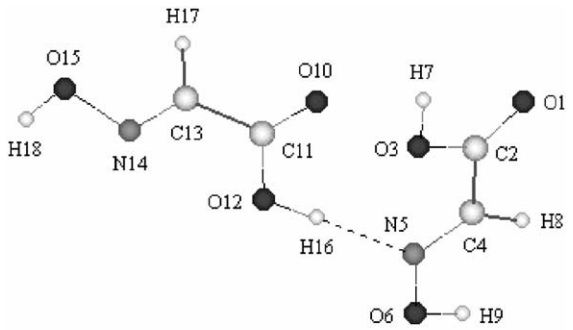

II

Fig. 4. Dimer II of the glyoxilic acid oxime.

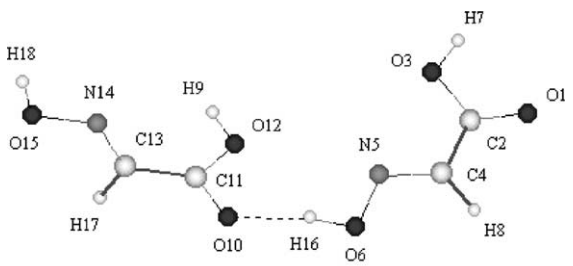

III

Fig. 5. Dimer III of the glyoxilic acid oxime.

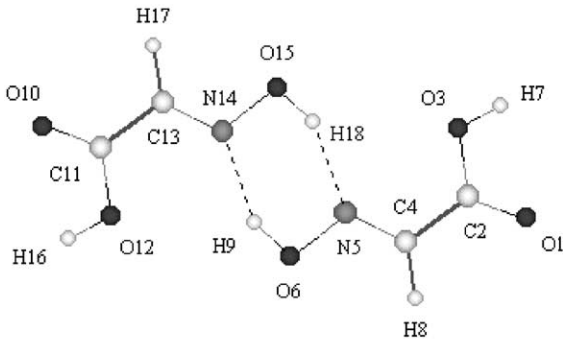

IV

Fig. 6. Dimer IV of the glyoxilic acid oxime.

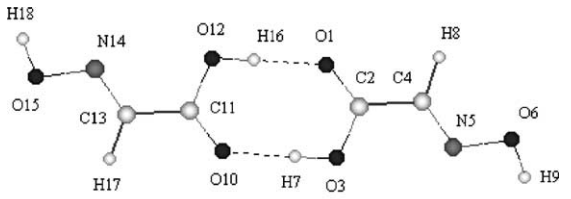

V

Fig. 7. Dimer V of the glyoxilic acid oxime.

6-31++G** level and 17–36% of the H-bonding energy at B3LYP/6-31G* level.

First, dimer II (with one N···H—O, Fig. 4) and dimer III (with one O···H—O hydrogen bond, Fig. 5) were considered. The sum of the H-bonding energy of II and III can be compared to the H-bonding energy of I. Since I contains one N···H—O and one O···H—O interactions this provides a test of the additivity of the individually determined N···H—O (from II) and O···H—O (from III). As seen from the results in Table 3, at B3LYP/6-31G* level, the hydrogen-bonding energy of I (−55.87 kJ/mol) was lower than the sum of the hydrogen-bonding energy estimated from II (−17.5 kJ/mol) and III (−25.94 kJ/mol) by −12.43 kJ/mol. The difference thus obtained could be attributed to the cooperativity in the cyclic dimer I, E^{coop} (dimer I). Further, using the same procedure the cooperative contribution in the cyclic tetramer was evaluated, E^{coop} (tetramer). The value thus obtained (−42.08 kJ/mol) is much lower as compared to that obtained for dimer I (−12.43 kJ/mol) and may explain the formation and the stability of the tetramer complex. Since the tetramer contains four identical seven-membered rings its cooperativity could be estimated from the cooperativity obtained for one seven-membered ring $4 \times E^{coop}$ (dimer I). The value thus obtained ($-49.72 = 4 \times -12.43$ kJ/mol) is lower as compared to that obtained using the first procedure mentioned above (E^{coop}(tetramer) = −42.08 kJ/mol).

The B3LYP/6-31++G** calculations predicted different cooperative contribution for dimer I (E^{coop}(dimer I) = −8.85 kJ/mol). To estimate the

Table 3
Hydrogen-bonding energies (ΔE, kJ mol^{-1}) of GAO dimers and tetramer

Method	System	ΔE_{uncorr}	ΔE^{h}	ΔE^{cp}	ΔE_{corr}	ΔH_{calc}
B3LYP/6-31++G**	Dimer I	−63.12	−57.31	−59.26	−53.45	−53.19
	Dimer II	−25.56	−22.62	−22.54	−19.6	−16.91
	Dimer III	−31.47	−27.45	−28.99	−24.97	−22.71
	Dimer IV	−55.07	−48.9	−51.34	−45.17	−44.61
	Dimer V	−67.82	−63.06	−63.83	−59.07	−58.68
	Tetramer	−253.28	−231.16	−236.23	−214.11	−197.22
B3LYP/6-31G*	Dimer I	−76.34	−70.32	−61.89	−55.87	−55.63
	Dimer II	−32.18	−28.99	−20.69	−17.5	−14.7
	Dimer III	−38.33	−34.08	−30.19	−25.94	−23.80
	Dimer IV	−67.26	−60.74	−55.46	−48.94 (−24.47)[a]	−48.51
	Dimer V	−80.99	−76.04	−64.37	−59.42 (−29.71)[a]	−58.94
	Tetramer	−297.06	−274.86	−238.04	−215.84	−198.74

E^{cp}: cp-corrected electronic hydrogen-bonding energy; E^{h}: harmonically zero point hydrogen-bonding energy.
[a] Half of the hydrogen-bonding energy.

tetramer cooperativity at B3LYP/6-31++G** level of the theory we applied the same two procedures mentioned above. The values thus obtained (E^{coop} (tetramer) = −35.83 kJ/mol) and ($4 \times E^{coop}$ (dimer I) = −35.40 kJ/mol) differ by −0.43 kJ/mol ($\Delta E^{coop} = E^{coop}(\text{tetramer}) - 4 \times E^{coop}(\text{dimer I})$) and indicate additional stabilization due to the formation of cyclic structure of the tetramer.

Another method to estimate the N···H—O and the O···H—O interactions in I involves consideration of cyclic dimers IV (with two N···H—O hydrogen bonds in the six-membered ring, Fig. 6) and V (with two O···H—O hydrogen bonds in the eight-membered ring, Fig. 7). Thus, the sum of the half of the interaction energy of IV and the half of the interaction energy of V can be compared to the H-bonding energy of I. However, the N···H—O and O···H—O bonding energies determined from the cyclic dimers IV and V should be compared with caution with those obtained from dimers II and III. Both IV and V dimers are cyclic and the determined from them individual H-bonding energies of N···H—O and O···H—O contain stabilization due to the cooperative interaction. Thus, it is expected that the second method will give lower N···H—O and O···H—O bonding energies (IV, −24.47 kJ/mol and V, −29.71 kJ/mol) as compared to the values determined applying the first one (II, −17.50 kJ/mol and III, −25.94 kJ/mol). Although the N···H and O···H bonding energies, obtained from IV and V, contain the cooperative contributions, their sum (−54.18 kJ mol^{-1}) is higher than H-bonding energy of dimer I (−55.87 kJ mol^{-1}). This result indicates that there is additional stabilization in the seven-membered ring of the cyclic dimer I.

To gain a deeper insight into the magnitude of the intermolecular interactions that bind the monomer units in the GAO tetramer we have to consider all types of the hydrogen bonding. There are three possible bonding types for ectt monomer in a cyclic dimer: head-to-tail (dimer I), head-to-head (dimer V) and tail-to-tail (dimer IV). As seen from Table 3, the lowest hydrogen-bonding energy was calculated for the head-to-head bonding type, −59.42 kJ/mol, as it is in dimer V. However, this bonding type was not observed in the crystal. To understand why the head-to-tail bonding type was realized (as it is in dimer I, −55.87 kJ/mol and in tetramer) but not the head-to-head one (that with the lowest bonding energy, −59.42 kJ/mol), we compared the bonding energies of dimer I aggregates from one side and of dimer V aggregates from the other side. In the first type aggregate similar to the crystalline arrangement, each GAO monomer forms two pairs head-to-tail H-bonding (each pair includes one O···H—O and one N···H—O). On the other hand, in an aggregate, constructed from dimers analogous to dimer V, each GAO monomer forms one pair head-to-head bonding (includes two O···H—O) and an other pair (includes two N···H—O) tail-to-tail H-bonding. The comparison of head-to-tail bonding energy (twice the hydrogen-bonding energy of I, −111.74 kJ/mol) with the sum of the hydrogen-bonding energies of head-to-head and tail-to-tail bonding types (the sum of H-bonding energy of IV and V, −108.36 kJ/mol) suggested that the aggregates of the head-to-tail hydrogen bonding are enthalpically preferred. This finding could explain the observed head-to-tail hydrogen bonding in the crystal structure of GAO.

From the calculations made it was possible to evaluate the total H-bonding energy in the seven-membered ring in dimer I and tetramer but not the individual O···H—O and N···H—O bonding energies. Thus, on the basis of these calculations we were not able to make suggestion about the individual N···H—O and O···H—O bonding strengths in the complexes studied. To this end, we have used the correlation between the H-bonding energy and the N···O and O···O distances, reported in the literature for many H-bonded systems [31,32]. We have compared the calculated N···O and O···O distances in I, II, III, IV and V (Table 4). As seen from Table 4, the O···O distance in I is between the corresponding ones in III and V. Thus, the O···H—O bonding energy of I could be expected between −25.94 kJ/mol (III) and −29.71 kJ/mol (V). The N···O distance in dimer I is close to that in dimer IV and the N···H—O bonding energy in dimer I could be approximately estimated of ∼−24.47 kJ/mol (IV). As compare to dimer I, in tetramer the O···O distances were calculated longer and the N···O distances were shorter. Since the N···O distance in tetramer is

Table 4
Intermolecular bond distances (Å) and corrected hydrogen-bonding energies (kJ mol^{-1}) of GAO dimers (I–V) and tetramer

Method	System	R(O···O)	R(N···O)	ΔE_{corr}
B3LYP/6-31G*	Dimer I	2.6957	2.8171	−55.87
	Dimer II	–	2.9477	−17.5
	Dimer III	2.7977	–	−25.94
	Dimer IV	–	2.8145	−48.94 (−24.47)[a]
	Dimer V	2.6894	–	−59.42 (−29.71)[a]
	Tetramer	2.7177	2.7868	−215.84
		2.7209	2.7812	
		2.7298	2.7755	
		2.7204	2.7811	

[a] Half of the hydrogen-bonding energy.

shorter than that in dimer IV it is expected that the N···H—O energy in tetramer should be lower than −24.47 kJ/mol. Thus, one may suggest that the N···H—O bonding energy in tetramer approaches the O···H—O one and both are relatively strong.

3.4. Natural population analysis of the dimer and tetramer

NPA of the monomer, dimer I and tetramer can give some insight into the interaction taking place upon aggregation. Natural population analysis data (given in Table 5) showed that the free hydrogen atoms in dimer I, H7 and H18 (Fig. 3) are more positive (have lower NPA values, than those in monomer), which contribute to aggregation of two dimers in tetramer. However, the free carboxylic oxygen (O_1) and the oxime nitrogen (N_{14}) in dimer I, became less negative (by 0.006 e^- and 0.007 e^-, respectively) and thus from purely electrostatic arguments it is difficult to predict stabilization of the tetramer unit. At the same time, the less negativity of N_{14} and O_1 atoms correlates with their higher H-bond basicity, which suggests further aggregation of dimer I to tetramer [34].

Natural population analysis data were used to investigate the charge changes, which reflect the forces driving the formation of the hydrogen bonds in dimer I and tetramer. The calculated natural charges (q_i) for monomer and their changes in dimer I and tetramer, (Δq_i), are presented in Table 6. As seen from the results in Table 6, in dimer I (Fig. 3) significantly changed were only the charges of the atoms, involved in the seven-membered ring (they are noted by "c"). In the cyclic tetramer, where all —NOH and —COOH groups are involved in hydrogen bonding, all atomic charges were found significantly changed. The higher partial charges of the atoms in tetramer (as compared to those of dimer I) suggested a substantial electrostatic interaction, which stabilizes the tetramer species in addition.

3.5. AIM electron density at bond critical points

To obtain additional information about the strengths of the O···H and N···H hydrogen bondings in dimer I and tetramer we undertook AIM study of the electron density at bond critical points. Table 7 contains data about the electron density at H-bond critical points as well as data at

Table 5
Natural population analysis data (a.u.) at B3LYP/6-31G* level of the theory for GAO monomer and GAO dimer I

System	H(COOH)	O=	N	H(NOH)
Monomer (ectt)	0.500	8.582	7.075	0.500
Dimer I	0.494[a]	8.576[a]	7.068[a]	0.499[a]

[a] Values for not hydrogen-bonded atoms.

Table 6
Selected natural charges (q_i) of GAO monomer (at B3LYP/6-31G* level of the theory) and charge shifts (Δq_i) on dimerization and tetramerization

Atom[a]	Tetramer Δq_i[b] (e)	Dimer I Δq_i[b] (e)	Monomer (ectt) q_i (e)
O_1	−0.058	0.006	−0.582
O_{10}	−0.059	−0.064[c]	
N_5	−0.049	−0.052[c]	−0.075
N_{14}	−0.049	0.007	
O_6	0.017	0.012	−0.550
O_{15}	0.017	0.003	
H_7	0.021	0.005	0.500
H_{16}	0.020	0.017[c]	
H_9	0.020	0.019[c]	0.500
H_{18}	0.020	0.001	

[a] See Figs. 1–3 for numbering of atoms.
[b] $\Delta q_i = q_i^{\text{complex}} - q_i^{\text{monomer}}$ (complex = dimer or tetramer).
[c] Values of atoms, included in the hydrogen-bonded ring of GAO dimer I.

the H–O bonds in dimer I and tetramer. The O···H and N···H hydrogen bonds in dimer I and tetramer have properties typical of closed-shell interactions as hydrogen bonds – low ρ_b and positive $\nabla^2\rho_b$, whereas the H—O bonds have features typical for covalent interactions. A trend of increasing ρ_b and $\nabla^2\rho_b$ at H-bond critical points with increasing H-bond strength was first noted by Carroll and Bader [35] and it was later confirmed by other authors [36,37]. A relationship between the depletion of ρ_b at H—O bond on complexation and the H-bond strength was also found [36]. Going from dimer I to tetramer, the AIM analysis showed that: (1) ρ_b and $\nabla^2\rho_b$ values at the $O_{10}\cdots H_9$ hydrogen bond critical point and depletion of ρ_b at H_9—O_6 bond decrease; (2) ρ_b and $\nabla^2\rho_b$ values at the $N_5\cdots H_{16}$ hydrogen bond critical point and depletion of ρ_b at H_{16}—O_{12} bond increase. Thus, the calculated properties of electron density at bond critical points for the species studied, indicated that as compared to dimer I, in tetramer the O···H bonds are weaker, while the N···H bonds are stronger. The result thus obtained is in full agreement with the experimental and calculated longer O···O (O···H) and shorter N···O (N···H) distances in tetramer as compared to dimer I (Table 1). It is however, interesting to compare the electron density properties of homo- O···H—O and hetero-nuclear N···H—O bondings first in dimer I, and second in tetramer. It was recently shown that ρ_b (X···H—A) and $\Delta\rho$ (H—A) reflect relatively small changes accompanying the H-bonding strength and they are comparable to different H-bond types [34]. The ρ_b ($O_{10}\cdots H_9$), ρ_b ($N_5\cdots H_{16}$), $\Delta\rho_b$ (H_9—O_6) and $\Delta\rho_b$ (H_{16}—O_{12}) values in dimer I confirmed the suggestion for stronger O···H hydrogen bond as compared to the N···H one. As seen from Table 7, these values in tetramer are in agreement with the suggestion made in Section 3.3, that the N···H—O bonding strength in tetramer approaches the O···H—O one.

On the basis of the calculated AIM ellipticity an attempt was made to estimate the π-delocalization in dimer I and tetramer. The ellipticity changes for dimer I and tetramer are presented in Table 8. In

Table 7
Selected bond critical point properties[a] (au) for GAO monomer, dimer I and tetramer (obtained at B3LYP/6-31G* level of the theory)

Bond[b]	Tetramer		Dimer I		Monomer	
	$\rho_b/\Delta\rho_b$[c]	$\Delta^2\rho_b/\Delta(\nabla^2\rho_b)$[d]	$\rho_b/\Delta\rho_b$[c]	$\nabla^2\rho_b/\Delta(\nabla^2\rho_b)$[d]	ρ_b	$\nabla^2\rho_b$
$(O_{10}\cdots)H_9$—O_6	0.319/−0.030	−1.688/0.186	0.317/−0.032	−1.666/0.208	0.349	−1.874
$(N_5\cdots)H_{16}$—O_{12}	0.304/−0.034	−1.550/0.234	0.307/−0.031	−1.571/0.213	0.338[e]	−1.784[e]
$O_{10}\cdots H_9$	0.0405	0.1259	0.0437	0.1361		
$N_5\cdots H_{16}$	0.0414	0.1103	0.0391	0.1042		

[a] ρ_b is the value of the electron density at the bond critical point, $\nabla^2\rho_b$ is the second derivative of the electron density (density Laplacian).
[b] See Figs. 1–3 for numbering of atoms.
[c] $\Delta\rho_b = \rho_b^{\text{complex}} - \rho_b^{\text{monomer}}$ (complex = tetramer or dimer).
[d] $\Delta(\nabla^2\rho_b) = \nabla^2\rho_b^{\text{complex}} - \nabla^2\rho_b^{\text{monomer}}$ (complex = tetramer or dimer).
[e] The values refer to H_3—O_7 bond of GAO monomer, Fig. 1.

Table 8
Selected AIM ellipticities (a.u.) at the bond critical points for GAO monomer (at B3LYP/6-31G* level of the theory) and ellipticity changes, $\Delta\varepsilon_i$,[a] on dimerization and tetramerization

Bond[b]	$\Delta\varepsilon_i^{\text{tetramer}}$	$\Delta\varepsilon_i^{\text{dimerI}}$	$\varepsilon_i^{\text{monomer}}$
C_2═O_1	−0.02	0.00	0.12
C_{11}═O_{10}	−0.02	−0.02[c]	
O_3—C_2	0.02	0.00	0.01
O_{12}—C_{11}	0.02	0.02[c]	
C_4—C_2	0.01	0.01	0.14
C_{13}—C_{11}	0.01	0.00	
O_6—N_5	0.02	0.02[c]	0.03
O_{15}—N_{14}	0.02	0.00	

[a] $\Delta\varepsilon_i = \varepsilon_i^{\text{complex}} - \varepsilon_i^{\text{monomer}}$ (complex = tetramer or dimer I).
[b] See Figs. 1–3 for atom numbering.
[c] Values of atoms, included in the hydrogen bonded ring of dimer I.

dimer I, the AIM ellipticity values showed π-delocalization only in the hydrogen-bonded ring. This ring involves six π-electrons and thus, additional stabilization of dimer I due to the aromaticity of hydrogen-bonded ring is possible [38]. The calculated ellipticities for all O—C, C—C, O—N bonds in the cyclic tetramer were found higher (positive $\Delta\varepsilon_i$ values) and that for C═O bond was lower (negative $\Delta\varepsilon_i$ value). The results thus obtained indicated π-delocalization over all atoms in the tetramer chain, which stabilize the cyclic tetramer unit in addition. The lowering of the ε(C═O) values is in agreement with the calculated longer C═O bonds in tetramer. At the same time, the higher ε values for C—O, C—C and O—N bonds corresponded to shorter bond lengths in tetramer. These findings indicated absence of pure single and pure double bonds in tetramer.

3.6. Vibrational study

Changes were observed in the calculated vibrational spectrum of GAO going from monomer to dimer I and tetramer and they may confirm the conclusions made on the basis of the calculated hydrogen-bonding energies. Vibrational frequencies of the monomer, three dimers and hydrogen-bonded tetramer were calculated using B3LYP/6-31G* method. The calculated changes of the most sensitive to aggregation vibrational frequencies ($\Delta\nu^{\text{scal}}$) are presented in Table 9. As seen from Table 9, due to the participation of the —NOH and —COOH groups in hydrogen bonds, $\nu(\text{O—H})_{\text{COOH}}$ and $\nu(\text{O—H})_{\text{NOH}}$ in dimer II (with one N···H bond, Fig. 4) and III (with one O···H bond, Fig. 5), showed a negative shifts, 219 and 235 cm^{-1}. In the cyclic aggregates, dimer I and tetramer, the calculated negative shift values for $\nu(\text{O—H})_{\text{COOH}}$ and $\nu(\text{O—H})_{\text{NOH}}$ are much higher, 433 and 505 for dimer I and 406 cm^{-1} and 535 cm^{-1} for tetramer. The higher vibrational shifts obtained for the cyclic dimer I and tetramer provide additional evidence for the substantial cooperativity in the cyclic structures. The calculated values suggested the presence of relatively strong O···H—O and N···H—O hydrogen-bond interactions in dimer I and tetramer. The ν(C═O) mode is also sensitive to aggregation and negative shift was calculated (57 cm^{-1} for dimer I and 51

Table 9
Selected calculated changes in the IR frequencies (cm^{-1}) from GAO monomer to dimer I, dimer II, dimer III, and tetramer

Vibrational mode	$\Delta\nu^{\text{scal}}$			
	Tetramer	Dimer I	Dimer II	Dimer III
$\nu(\text{OH})_{\text{NOH}}$	−406	−433	32	−235
$\nu(\text{OH})_{\text{COOH}}$	−535	−505	−219	−7
ν(C═O)	−51	−57	−21	−30
ν(CO)	70	96	–	11
ν(NO)	84	78	12	–
$\delta(\text{NOH})_{\text{i.p.}}$	97	120	1	73
$\delta(\text{NOH})_{\text{o.p.}}$	350	310	−33	270
$\delta(\text{COH})_{\text{i.p.}}$	107	105	57	18
$\delta(\text{COH})_{\text{o.p.}}$	338	321	198	10

cm^{-1} for tetramer). As seen from Table 9, the calculated ν(CO) and ν(NO) vibrations are shifted to higher frequencies in the cyclic aggregates. Changes were observed in the deformation mode positions as well. The most sensitive to the N···H—O and O···H—O hydrogen bondings are δ(NOH) and δ(COH) deformation modes (especially out-of-plane NOH and COH) (Table 9).

4. Conclusion

Our calculations showed that both B3LYP/6-31G* and B3LYP/6-31++G** levels of the theory described correctly the geometry of the cyclic GAO tetramer. The calculated thermodynamic parameters of the intermolecular hydrogen-bonding interactions in the cyclic dimer I and tetramer showed higher free energy stabilization of tetramer, although the last one was entropically unfavored. The lower incremental hydrogen-bonding energy obtained for the second hydrogen bonding indicated that the formation of larger than dimer aggregate for GAO is enthalpically favored. The comparative study of chain aggregate with both head-to-head and tail-to-tail bondings and chain aggregate only with head-to-tail bondings, showed that the latter is enthalpically preferred in agreement with the crystal structure of GAO. The calculated H-bonding energies of various dimers suggested that there is a cooperative contribution to the stabilization of the cyclic dimer I and tetramer. The lower total cooperative energy for the cyclic tetramer (E^{coop}(tetramer) = −42.08 kJ/mol) in comparison with that for dimer I (E^{coop}(dimer I) = −12.43 kJ/mol) confirmed the aggregation and explained the tetramer formation in the crystal. The calculated N···O and O···O distances and hydrogen-bonding energies showed that the N···H—O bonding energy in tetramer approaches the O···H—O one. Both H-bonds in GAO tetramer were estimated as relatively strong (O···H—O between −25.94 and −29.71 kJ/mol and N···H—O less than −24.47 kJ/mol). The calculated $\Delta\nu$(OH) values are in agreement with this prediction. The high shifts of the most sensitive to aggregation vibrations (O—H stretching, NOH and COH out-of-plane bending) confirmed the cooperative effect in the cyclic structures. The higher partial charges of all atoms (which suggested a substantial electrostatic interaction) as well as the higher electronic π-delocalization in tetramer as compared to cyclic dimer I, explained the tetramer preference in the crystal structure.

Acknowledgements

Financial support from the Technical University of Vienna is greatly acknowledged. The authors thank the Computer Center of the Technical University of Vienna and Prof. Dr. Hans Mikosch for the computational facilities and the services provided. We are grateful to Dr. Dodoff for the help in obtaining of GAO crystals.

References

[1] N. Trendafilova, G. Bauer, I. Georgieva, N. Dodoff, Spectrochim. Acta 55 (1999) 2849.
[2] H. Wieland, Berg 43 (1910) 3363.
[3] N. Trendafilova, G. Bauer, I. Georgieva, V. Delchev, J. Mol. Struct. 604 (2–3) (2002) 211.
[4] K. Mereiter, Private Communication.
[5] L. Turi, J.J. Dannerberg, J. Am. Chem. Soc. 116 (1994) 8714.
[6] L. Turi, J.J. Dannerberg, J. Phys. Chem. 96 (1992) 5819.
[7] L. Turi, J.J. Dannerberg, J. Phys. Chem. 97 (1993) 12197.
[8] L. Turi, J.J. Dannerberg, J. Phys. Chem. 100 (1996) 9638.
[9] G.I. Cardenas-Jiron, A. Masunov, J.J. Dannenberg, J. Phys. Chem. 103 (1999) 7042.
[10] M.J. Frisch et al., GAUSSIAN 98, A.7, Gaussian Inc., Pittsburgh, PA, 1998.
[11] C. Lee, W. Yang, R.G. Parr, Phys. Rev. B 37 (1988) 785.
[12] A.D. Becke, J. Chem. Phys. 98 (1993) 5648.
[13] J.J. Novoa, C.J. Sosa, J. Phys. Chem. 99 (1995) 15837.
[14] D.R. Mamann, Phys. Rev. B (1997) R10157.
[15] C. Maerker, P.v.R. Schleyer, K.R. Liedl, T.-K. Ma, M. Quack, M.A. Suhn, J. Comp. Chem. 18 (1997) 1695.
[16] M. Lonzynski, D. Rusinska-Raszak, H.-G. Mack, J. Phys. Chem. A 102 (1998) 2899.
[17] (a) S.F. Boys, F. Bernardi, Mol. Phys. 19 (1970) 553; (b) A. Meunier, B. Levy, G. Bertier, Theor. Chim. Acta 29 (1973) 49.
[18] I. Mayer, P.R. Surjan, Chem. Phys. Lett. 191 (1992) 497.
[19] L. Turi, J.J. Dannenberg, J. Phys. Chem. 97 (1993) 2488.
[20] S. Simon, M. Duran, J.J. Dannenberg, J. Phys. Chem. A 103 (1999) 1640.
[21] L.A. Curtiss, J. Chem. Phys. 67 (1977) 1144.
[22] L.A. Curtiss, D.J. Frurip, M. Blander, J. Am. Chem. Soc. 100 (1978) 79.

[23] D.J. Frurip, L.A. Curtiss, M.J. Blander, J. Am. Chem. Soc. 102 (1980) 2610.
[24] R.F.W. Bader, S.G. Anderson, A.J. Duke, J. Am. Chem. Soc. 101 (1979) 1389.
[25] R.F.W. Bader, T.S. Slee, D. Cremer, E. Kraka, J. Am. Chem. Soc. 105 (1983) 5061.
[26] R.F.W. Bader, P.J. MacDougall, J. Am. Chem. Soc. 107 (1985) 6788.
[27] R.F.W. Bader, Atoms in Molecules, Oxford University Press, New York, 1990.
[28] A. Destexhe, J. Smets, L. Adamowicz, G. Maes, J. Phys. Chem. 98 (1994) 1506.
[29] Y. Dimitrova, Spectrochim. Acta Part A 57 (2001) 2457.
[30] G.A. Jeffrey, An Introduction of Hydrogen Bonding, Oxford University Press, New York, 1997.
[31] P. Gilli, V. Bertolasi, V. Ferretti, G. Gilli, J. Am. Chem. Soc. 116 (1994) 909.
[32] G. Gilli, P. Gilli, J. Mol. Struct. 552 (1–3) (2000) 1.
[33] Y. Dimitrova, S.D. Peyerimhoff, J. Phys. Chem. 97 (1993) 12731.
[34] J.A. Platts, Phys. Chem. Chem. Phys. 2 (2000) 3115.
[35] M.T. Carroll, R.F.W. Bader, Mol. Phys. 63 (1988) 387.
[36] J.A. Platts, S.T. Howard, B.R.F. Bracke, J. Am. Chem. Soc. 118 (1996) 2726.
[37] J. Luis Perez-Lustres, M. Bräuer, M. Mosquera, T. Clark, Phys. Chem. Chem. Phys. 3 (2001) 3569.
[38] J.J. Dannenberg, R. Rios, J. Phys. Chem. 28 (1994) 6714.